MOLECULAR AND CELLULAR BIOLOGY, Mar. 1997, p. 1490–1502 Vol. 17, No. 3
0270-7306/97/$04.00+0
Copyright © 1997, American Society for Microbiology

bic, a Novel Gene Activated by Proviral Insertions in Avian Leukosis Virus-Induced Lymphomas, Is Likely To Function through Its Noncoding RNA

WAYNE TAM,[1,2*†] DINA BEN-YEHUDA,[2‡] AND WILLIAM S. HAYWARD[1,2]

Graduate Program in Molecular Biology, Cornell University Graduate School of Medical Sciences,[1] and Molecular Biology Program, Sloan-Kettering Institute for Cancer Research, Memorial Sloan-Kettering Cancer Center,[2] New York, New York 10021

Received 16 August 1996/Returned for modification 10 October 1996/Accepted 9 December 1996

The *bic* locus is a common retroviral integration site in avian leukosis virus (ALV)-induced B-cell lymphomas originally identified by infection of chickens with ALVs of two different subgroups (Clurman and Hayward, Mol. Cell. Biol. 9:2657–2664, 1989). Based on its frequent association with c-*myc* activation and its preferential activation in metastatic tumors, the *bic* locus is thought to harbor a gene that can collaborate with c-*myc* in lymphomagenesis and presumably plays a role in late stages of tumor progression. In the present study, we have cloned and characterized two novel genes, *bdw* and *bic*, at the *bic* locus. *bdw* encoded a putative novel protein of 345 amino acids. However, its expression did not appear to be altered in tumor tissues, suggesting that it is not involved in oncogenesis. The *bic* gene consisted of two exons and was expressed as two spliced and alternatively polyadenylated transcripts at low levels in lymphoid/hematopoietic tissues. In tumors harboring *bic* integrations, proviruses drove *bic* gene expression by promoter insertion, resulting in high levels of expression of a chimeric RNA containing *bic* exon 2. Interestingly, *bic* lacked an extensive open reading frame, implying that it may function through its RNA. Computer analysis of RNA from small exon 2 of *bic* predicted extensive double-stranded structures, including a highly ordered RNA duplex between nucleotides 316 and 461. The possible role of *bic* in cell growth and differentiation is discussed in view of the emerging evidence that untranslated RNAs play a role in growth control.

The proto-oncogene c-*myc* plays a critical role in the development of lymphomas in birds and mammals (16, 48). Experiments in both the murine and avian systems indicate that activation of c-*myc* alone is not sufficient for full malignancy. In Eμ-c-*myc* transgenic mice, monoclonal lymphomas develop only after a variable and relatively long latency (2), suggesting that additional genetic alterations besides c-*myc* are required to induce full-blown lymphomas. Consistent with this notion, c-Myc (or the viral homolog v-Myc) is able to cooperate with a number of other proto-oncogene products in lymphomagenesis in rodents (1). These include the nuclear protein Bmi-1 (26, 27, 71), Ras G protein (3, 40, 60), the serine/threonine kinases Pim-1 (70, 72) and Raf (40), the nonreceptor protein-tyrosine kinase Abl (28, 41), and the mitochondrial membrane protein Bcl-2 (45, 62, 63).

In birds, studies of avian leukosis virus (ALV)-induced lymphomas have provided strong evidence for the requirement of multiple genetic events in lymphomagenesis. The development of avian lymphoid leukosis is believed to follow an orderly progression through three distinct clinical stages (15, 49). (i) Transformed follicles, which are hyperplastic follicles consisting of abnormally proliferating lymphoblasts, appear within 4 to 8 weeks postinfection, and an estimated 10 to 100 transformed follicles can be found in a single bursa. (ii) From 10 to 14 weeks postinfection onwards, macroscopic tumor nodules appear in the bursa. If present at all, they occur either singly or rarely as a pair in any one bursa. Most of the other transformed follicles regress along with other elements of the bursa. (iii) Finally, about 4 to 8 months postinfection, metastasis occurs from the bursa to visceral organs, predominantly the liver, resulting in massive lymphomatosis and death of the host.

Integrations at the c-*myc* locus are found at similar high frequencies in primary (bursal) and metastatic tumors (29), as well as in transformed follicles (20). Thus, insertional activation of c-*myc* appears to be an early event in avian lymphoid leukosis. Transplantation of 18-day embryonic bursal cells infected in vitro with HB-1, an avian retrovirus carrying a recombinant *myc*, into embryos with chemically ablated bursal follicles results in the formation of transformed follicles within the reconstituted bursae (47, 66), implying that c-*myc* activation is sufficient for the generation of transformed follicles. Transformed follicle formation, however, is necessary but not sufficient for development of avian leukosis (6). In the bursal reconstitution system, only a portion of the transformed follicles generated by in vitro HB-1 infection progress to form bursal lymphomas with a relatively long latency (66). These observations strongly imply that additional genetic events besides c-*myc* activation are necessary for a fully malignant state.

To identify the genetic events necessary for inducing tumor progression in ALV-induced lymphomas, Clurman and Hayward (14) used a double-infection protocol designed to increase the incidence of multiple insertional mutations. This protocol involved sequential infection of chickens with ALV of two different subgroups. Twelve-day chicken embryos were first infected with UR2AV′, a subgroup A ALV, and were subsequently infected with RAV-2, a subgroup B ALV, 14 days after the initial infection. The use of ALVs of two different

* Corresponding author. Mailing address: Sloan-Kettering Institute for Cancer Research, Memorial Sloan-Kettering Cancer Center, Box 46, 1275 York Ave., New York, NY 10021. Phone: (212) 639-8188. Fax: (212) 746-8624. E-mail: wtam@mail.med.cornell.edu.

† Present address: Department of Pathology, The New York Hospital—Cornell Medical Center, New York, NY 10021.

‡ Present address: Department of Hematology, Hadassah University Hospital, Jerusalem, Israel.

subgroups enabled superinfection to occur. The time span between these two infections facilitated a second insertional mutagenesis event by allowing clonal expansion of cells which have sustained the first mutational event, for example, c-*myc* activation, upon the initial infection. Using this approach, a novel common retroviral integration site, termed *bic*, was identified. Proviral integrations at the *bic* locus are found frequently in conjunction with c-*myc* activation and the frequency of *bic* integrations is higher in metastatic tumors than in primary tumors (14), suggesting that proviral integrations at *bic* activate a cellular gene that can collaborate with c-*myc* in lymphomagenesis and that is involved in late stages of tumor progression in these lymphomas.

In the present study, we describe the isolation of a novel gene that appears to be expressed specifically in lymphoid/hematopoietic tissues. Its expression is activated by promoter insertion at the *bic* locus. Interestingly, it lacks an extensive open reading frame (ORF) and is predicted to form strong secondary structures. The possibility that *bic* acts as a novel *myc* collaborator by functioning as a noncoding RNA is discussed in view of the emerging role of untranslated RNAs in cell growth and tumorigenesis.

MATERIALS AND METHODS

Chicken tumors. Chicken tumors analyzed in this study were generated from the double infection experiments described previously (14). 465L and 705L are metastatic lymphomas in livers (L) from birds 465 and 705, respectively. 451Sp is a metastatic lymphoma in spleen (Sp) from bird 451. Tumors 465L, 705L, and 451Sp all contain proviral integrations at *bic* and c-*myc*. 429L, 420L, and 708L are metastatic lymphomas in livers from birds 429, 420, and 708, respectively. Tumors 429L, 420L, and 708L do not harbor proviral integrations at *bic*. 429L, however, contains a c-*myc* integration; 420L and 708L have c-*myb* integrations.

Genomic cloning and restriction mapping. A genomic library from *Bgl*II-digested DNA from normal chicken erythrocytes (RBC) was prepared as follows: chicken RBC DNA was digested to completion with *Bgl*II and size fractionated on a 10 to 40% sucrose gradient. Fractions containing DNA of sizes 15 to 20 kb, which hybridized strongly to the 1.6-kb *Pvu*II-*Eco*RI (PR) genomic probe (14) on Southern analysis, were pooled and ligated to λ DASHII arms doubly digested with *Bam*HI and *Hin*dIII (Stratagene) and packaged by using Gigapack II Gold packaging extracts (Stratagene). About 60,000 plaques were screened with the PR probe. One positive clone (λ20.9; see Fig. 1a) was isolated and was restriction mapped by partial digestion of the λ insert by using a variety of restriction enzymes.

Northern blot analysis. Total RNA was extracted from tissues by using RNAzol B (Biotecx Laboratories, Inc.), which is modified from a single-step guanidinium isothiocyanate procedure for RNA isolation (11). Polyadenylated RNA was selected from total RNA by affinity chromatography on oligo(dT) columns. Total RNA (20 μg) or poly(A)$^+$ RNA (1 to 5 μg) was electrophoresed in 1.2% agarose–6% formaldehyde in 0.2 M MOPS, 5 mM sodium acetate, 1 mM EDTA, pH 7.0, and transferred to nitrocellulose (Schleicher & Schuell, Inc.). Nitrocellulose filters were hybridized under stringent conditions to radioactively labeled DNA or RNA probes. For hybridization to DNA probes, filters were prehybridized for 2 to 3 h in a solution containing 50% formamide, 5× SSC (1× SSC is 0.15 M NaCl plus 0.015 M sodium citrate), 5× Denhardt solution, 1% sodium dodecyl sulfate (SDS), and 100 to 200 μg of sonicated salmon sperm DNA per ml at 42°C and hybridized overnight under the same conditions to 2×10^6 to 4×10^6 cpm of ^{32}P-labeled random-primed DNA probes per ml. Blots were then washed twice for 15 min at room temperature in 2× SSC–0.5% SDS and twice for 15 min at 55°C. A final wash was performed at 60°C for 30 min in 0.1× SSC–0.1% SDS. For hybridization to RNA probes, filters were prehybridized and hybridized in a solution containing 50% formamide, 6× SSC, 1% SDS, 0.1% Tween 20, and 100 μg of tRNA per ml at 55°C and hybridized overnight under the same conditions to 2×10^6 to 4×10^6 cpm of ^{32}P-labeled RNA probes per ml generated in vitro from linearized plasmids. Blots were washed twice for 30 min at room temperature in 1× SSC–0.1% SDS and 30 min at 65°C in 0.1× SSC–0.1% SDS. Genomic fragments isolated from p415LNC (14) (see Fig. 1a) and subclones of λ20.9 were used as probes in Northern analysis. Probes A, B, C, D, E, F, G, H, I, J, K, and 1.9 X-B (see text and Fig. 1a) correspond to the following restriction fragments, respectively: 0.5-kb *Xba*I-*Hin*cII; 0.4-kb *Hin*cII-*Pst*I; 0.6-kb *Pst*I-*Bam*HI; 0.6-kb *Bam*HI-*Eco*RI; 0.9-kb *Eco*RI-*Xba*I; 0.6-kb *Xba*I-*Sac*I; 2.6-kb *Bgl*II; 1.4-kb *Bgl*II; 1.4-kb *Eco*RI-*Bam*HI; 0.7-kb *Bam*HI-*Xba*I; 1.8-kb *Sac*I; and 1.9-kb *Xba*I-*Bam*HI. Probes A, B, C, D, E, F, I, and J were used in the form of RNA probes, and probes G, H, and K were used as DNA probes. The *bic* cDNA probe used in Fig. 4a was a 0.8-kb artificially constructed *bic* cDNA spanning *bic* exon 1 and exon 2a.

cDNA cloning. The tumor cDNA library was custom prepared from 5 μg of poly(A)$^+$ RNA from lymphoma 705L by Invitrogen (San Diego, Calif.). A total of 5×10^5 clones were screened with probes A, B, and C (see Fig. 1a) by using standard procedures. Briefly, the bacteria were plated onto 10 15-cm L-broth agar plates containing 50 μg of ampicillin per ml and 25 μg of tetracycline per ml, grown overnight at 37°C, and overlaid with nitrocellulose filters. Duplicate filters were made for each plate. The bacterial colonies were lysed by wetting the filters in 0.5 M NaOH–1.5 M NaCl for 5 min followed by neutralization in 1.5 M NaCl–0.5 M Tris (pH 7.4) for 5 min. The filters were finally wetted in 2× SSC and baked for 2 h in a vacuum oven after air drying. Prehybridization and hybridization of the filters were as described previously (42). The λgt10 spleen cDNA library was purchased from Clontech (Palo Alto, Calif.). A total of 2×10^6 recombinant phages were screened with either probe A or probe C. Library screening was performed as recommended by the manufacturer with RNA probes generated by in vitro transcription. Briefly, the phages were plated onto 50 15-cm L-broth agar plates with a lawn of *Escherichia coli* (C600hfl; Clontech) in 0.7% top agarose, grown overnight at 37°C, and overlaid with nitrocellulose filters for 3 min. The filters were then immersed in 1.5 M NaCl-NaOH, neutralized, and washed in 3× SSC. Duplicate filters were made for each plate. The filters were baked in a vacuum oven for 2 h at 80°C. They were then prehybridized in a solution containing 50% formamide, 6× SSC, 1% SDS, 0.1% Tween 20, and 100 μg of yeast tRNA for 3 to 5 h at 50°C and hybridized in the same solution with 0.5×10^6 to 1×10^6 cpm of ^{32}P-labeled probe per ml at 50°C for 18 to 20 h. A final wash was done at 60°C. Positive clones were subcloned into pBluescript SK$^+$ (Stratagene).

cDNA cloning by PCR. For 3′ rapid amplification of cDNA ends (RACE), first-strand cDNA was synthesized for 60 min at 42°C and 30 min at 48°C, with 1 μg of 465L poly(A)$^+$ RNA in a buffer containing 50 mM Tris (pH 8.3), 75 mM KCl, 3 mM $MgCl_2$, 1 mM dithiothreitol (DTT), 1 mM each deoxynucleoside triphosphate (dNTP), 1 U of RNasin (Promega) per μl, 10 U of Superscript II RT (Bethesda Research Laboratories [BRL]) per μl, and 0.5 μg of a $(dT)_{17}$-adaptor primer (5′GACTCGAGTCGACATCGAT$_{17}$3′) that contains three cloning sites 5′ of a stretch of T's. The cDNA pool was then diluted with TE. Then, 5 μl of the dilution of the cDNA pool was amplified by PCR under the following conditions. Amplification was in a volume of 100 μl containing 10 mM Tris (pH 8.5), 50 mM KCl, 3 mM $MgCl_2$, 0.001% (wt/vol) gelatin, 0.2 mM each dNTP, either primer A or B (0.25 μM; for a list of primers, see below), an adaptor primer), GACTCGAGTCGACATCG, 5 μl of the diluted cDNA pool, and 2.5 U of Amplitaq DNA polymerase (Perkin Elmer Cetus), overlaid with 50 μl of paraffin oil. All of the reaction components except the polymerase were premixed and heated at 80°C for 3 min, after which the enzyme was added and PCR cycling was started. The first amplification cycle consisted of 94°C for 5 min, 55°C for 5 min, and 72°C for 20 min. This was followed by 40 cycles of 94°C for 40 s, 55°C for 1 min, and 72°C for 3 min. PCR products were analyzed by agarose gel electrophoresis, and their specificities were evaluated by Southern blot analysis. Specific PCR products were filled in with Klenow fragment, digested by *Sal*I, purified on NuSieve agarose gels, and cloned into pBluescript SK$^+$.

5′ RACE was performed using a commercially available 5′ RACE kit from Clontech according to the manufacturer's recommendations, which were based on the SLIC procedure (19). First-strand cDNA was primed with a *bic* exon 2-specific primer, primer C, using 2 μg of poly(A)$^+$ RNA isolated from the bursa of a normal 10-week-old chicken. The cDNA pool was purified on a Geno-Bind column (Clontech), ethanol precipitated, and ligated to a single-stranded anchor oligonucleotide with T4 DNA ligase. The anchored products were then diluted 10-fold with 90 μl of TE, and 1 μl was used for a "hot start" PCR mixture containing 0.2 μM concentrations of an anchor primer and an upstream *bic* exon 2-specific primer (primer D) in the same PCR cocktail as described above, except that the final volume was 50 μl instead of 100 μl. Denaturation was for 45 s at 94°C, annealing was for 45 s at 60°C, and extension was for 2 min at 72°C, for 35 cycles. PCR products were then analyzed by gel electrophoresis and Southern blotting. To determine the structure of the larger 5′ RACE product (cN5′R-1), the PCR products from the first amplification were first purified by centrifugation on GlassMAX spin columns (BRL). Then, 1/10 of the purified products was used for reamplification with 0.25 μM concentrations of either anchor primer and primer E under the same reaction conditions as the first amplification or primer D and primer F under the following conditions: denaturation for 40 s at 94°C, annealing for 45 s at 53°C, and extension for 1 min at 72°C. Resulting products were separated on Nusieve agarose gels and cloned in pBluescript SK$^+$.

To obtain 5′ cDNAs from tumor transcripts, 1/5 of the first-strand cDNA pool obtained from reverse transcription of tumor poly(A)$^+$ RNA (described above) was ethanol precipitated and resuspended in 10 μl of TE. Then 1/2 of this sample was used in a hot-start PCR mixture containing 0.25 μM concentrations of a RAV-2 long terminal repeat U5-specific primer (primer G) and a *bic* exon 2a-specific primer (primer C) in the same PCR cocktail as described above. Denaturation was for 40 s at 94°C, annealing was for 1 min at 60°C, and extension was for 1 min 30 s at 72°C, for 35 cycles. Specificity of the products was evaluated by Southern analysis with a nested *bic* exon 2a primer and a primer in the leader region of RAV-2. Specific products were gel purified and cloned into pBluescript SK$^+$.

Sequences of the oligonucleotides used in PCR were as follows: primer A, TTCTGCAAACAGACGCAC; primer B, GGAACACTTGCTGCATAATCAC (intron primer); primer C, GCGTCTGTTTGCAGAACAAGCCATC; primer

D, TGTCACATGGAGGTCTTCTCAGCGTG; primer E, CCTCTGTTTTTTT TCCCCCTTGAG; primer F, CATGTGAGATGGAACAAAGGAAGTC; primer G, CGTTGATTCCCTGACGACGACTACG. All primers were purified by fast protein liquid chromatography (Pharmacia) and dissolved in TE.

Determination of allelic polymorphism using PCR. Normal muscle DNA (1 μg) from chicken 465 was subjected to PCR amplification with 0.25 μM concentrations of primer 1 and primer 2 (primer 1, CACTGCATACAGAGGAAA CTATG (intron primer); primer 2, CGATTAGCATTAACAACATACAGCC) in the same PCR cocktail as described previously. Denaturation was for 45 s at 94°C, annealing was for 1 min at 54°C, and extension was for 1 min at 72°C, for 35 cycles. The PCR products were subcloned in pBluescript SK^+.

Preparation of ^{32}P-labeled DNA and RNA probes. Radioactive DNA probes were generated by random priming (22). Radiolabeled RNA probes were generated by in vitro transcription from DNA cloned in pBluescript SK^+. Purified plasmids were completely linearized by the appropriate restriction enzymes. The samples were then treated with proteinase K, extracted with phenol/chloroform, ethanol precipitated, and resuspended in TE (pH 7.4) at a concentration of 1 μg/μl. The DNA templates were then used to generate RNA probes by in vitro transcription using an RNA transcription kit (Stratagene). The reaction was in a volume of 25 μl containing 40 mM Tris (pH 8.0); 8 mM $MgCl_2$; 2 mM spermidine; 50 mM NaCl; 0.25 mM each ATP, GTP, and CTP; 30 mM DTT; 20 U of RNasin (Promega); 80 to 125 μCi of [α-^{32}P]UTP (800 Ci/mmol; NEN); 10 U of T3 or T7 polymerase; and 1 μg of digested DNA template. Transcription was carried out at 37°C for 30 to 45 min. The DNA template was then removed by adding 10 U of RNase-free DNase (Stratagene) and incubating at 37°C for 15 min. For RNase protection assays, radiolabeled RNA was subsequently purified by phenol/chloroform extraction and ethanol precipitation. For Northern blots, 200 μl of RNA column buffer (10 mM Tris [pH 7.4], 1 mM EDTA, 0.1 M NaCl, 0.1% SDS, and 100 μg of tRNA per ml) was added to the reaction mixture after DNase treatment. The mixture was then run through a G50 Sephadex (Pharmacia) column equilibrated with the RNA column buffer. The probe was then used directly in Northern blots.

RNase protection assays. Total RNA (20 μg) was precipitated and resuspended in 30 μl of hybridization buffer (40 mM PIPES [pH 6.4], 1 mM EDTA, 0.4 M NaCl, 80% formamide) containing 150,000 cpm of RNA probe. RNA samples were then heated at 85°C for 10 min and incubated at 47°C overnight. Then, 300 μl of RNase digestion buffer (300 mM NaCl, 10 mM Tris-Cl [pH 7.4], 5 mM EDTA), containing RNase A (Sigma) and RNase T_1 (BRL) at concentrations of 40 μg/ml and 2,400 U/ml, respectively, was added and the reaction mixture was incubated at 34°C for 1 h. RNase digestion was terminated by incubating the reaction mixture for 30 min at 37°C after addition of SDS to 0.5% and proteinase K to 100 μg/ml. The reaction mixture was then phenol/chloroform extracted and precipitated with 2.5 vol of ethanol after the addition of 10 μg of carrier tRNA. The precipitate was resuspended in formamide loading buffer, denatured at 95°C for 5 min, and run on a 6% urea-acrylamide sequencing gel as described previously (42). The gel was fixed, dried, and exposed to film at −70°C. The RNA probe used for RNase protection was generated from the plasmid pHc-X.UE, which contains a PCR-generated partial cDNA spanning nucleotides 183 to 335 of *bic*.

Sequencing reactions. Sequencing of cDNA and genomic clones was performed on double-strand templates with synthetic primers. Reactions were performed with a Sequenase kit, version 2.0 (U.S. Biochemicals). Both strands were sequenced across all primer-binding sites.

Computer analysis. To search for sequencing homology, nucleotide and peptide sequence databases were screened by FASTA (51) and BLAST (4) programs. Protein motifs were searched by screening the PROSITE database (GCG software package). RNA secondary structure analysis was performed by the FOLDRNA (74) program (GCG software package). The resulting analysis was then displayed graphically.

RESULTS

Detection of transcripts at the *bic* locus. The genomic region spanning the integration cluster was previously cloned as a 7.5-kb *Eco*RI tumor-specific junction fragment, p415LNC (14). A 1.6-kb *Pvu*II-*Eco*RI cellular genomic fragment (PR) of this clone identified heterogeneous transcripts in the tumors with proviral integrations at the *bic* locus (14). Since avian retroviruses tend to activate cellular proto-oncogenes by promoter insertion (29, 69), it seems likely that the transcriptional unit, if any, affected by the proviral insertions would be located downstream of the integration cluster. To clone the genomic region downstream of the integration cluster, a chicken genomic library was screened with PR as a probe, and a 20.9-kb *Bgl*II-*Bgl*II genomic clone, λ20.9, was isolated. In order to detect transcripts within this genomic region, smaller subclones of λ20.9 (Fig. 1a) were used as probes on Northern blots containing poly(A)$^+$ or total RNAs from tumor and normal adult tissues. Three classes of transcripts were identified in this analysis. The first was detected by using genomic fragments isolated from the 5′ portion of λ20.9 (probes I and J), as well as probes G and H from p415LNC. These probes detected transcripts similar to those detected previously by using probe PR (14), which were tumor specific and had different sizes in different tumors (Fig. 1b). However, they appeared less heterogeneous than previously reported. Apparently, only probes downstream or spanning the integration site of the provirus (G, H, I, and J for 705L; I and J for 451Sp) were able to detect these transcripts. Interestingly, probe J was the most downstream genomic probe that hybridized to these transcripts. The sizes of the transcripts and their patterns of hybridization were consistent with their being read-through transcripts which initiated from the viral promoters and terminated within the 0.7-kb *Bam*HI-*Xba*I genomic fragment J. The second class consisted of two transcripts of about 2.6 and 1 kb, detected initially by a 1.9-kb *Xba*I-*Bam*HI genomic probe (1.9 X-B) located further downstream of the integration cluster. Most importantly, these two transcripts were overexpressed in tumors that harbored a proviral integration at *bic* (465L, 705L, and 451Sp) but were not detected in tumors which showed no gene rearrangements at the *bic* locus (429L and 420L) (Fig. 1c). Transcripts of similar sizes were also detected at very low abundances in adult chicken lymphoid tissues in Northern blots containing poly(A)$^+$ RNAs from a panel of normal chicken tissues (see below). To further characterize the structures of these two transcripts, we performed Northern blotting with smaller genomic fragments. While the shorter transcripts hybridized only to probe A, the longer transcript hybridized to probes A, B, C, and D (Fig. 1d), suggesting that these transcripts were derived from the same gene by alternative polyadenylation or splicing. The third class of transcripts was initially identified as a single 1.4-kb mRNA by using a 1.8-kb *Sac*I genomic fragment (probe K). This transcript was apparently not altered either quantitatively or qualitatively by proviral integrations at *bic* (Fig. 1e).

Cloning of the *bic* gene. Since the expression of the 2.6- and 1-kb transcripts was altered by proviral integrations at the *bic* locus, they most likely represent transcripts from the candidate *bic* gene. The cDNA sequences for the long and short transcripts of *bic* (bic_L and bic_S) were determined by both conventional cDNA screening and anchored-PCR procedures (see Materials and Methods). The structures of selected cDNAs are shown below the restriction map of *bic* in Fig. 2. A cDNA library derived from 705L (a metastatic lymphoma harboring a *bic* integration) RNA and a normal chicken spleen cDNA library were screened by using probes A, B, and C. From the tumor cDNA library, six overlapping clones were isolated and analyzed. Comparison of the restriction maps and sequences of these clones with those of the corresponding genomic regions showed that none of these represented spliced RNAs. The longest of these clones, cT12, extended colinearly with the genomic sequence from 100 bp downstream of the *Xba*I site to 282 bp downstream of the *Sac*I site, terminating with a poly(A) tail. Hybridization of contiguous genomic probes to the 2.6-kb transcript (Fig. 1d) indicated that cT12 was indeed derived from the 2.6-kb transcript. Based on RNase protection assays, the structures of *bic* transcripts in tumors and normal tissues were identical along the genomic region spanned by cT12 (data not shown). From the normal chicken spleen cDNA library, two positive clones, cN43.1 and cN48.1, were isolated. cN43.1 was nested within cT12. It was a 944-bp cDNA which possessed a poly(A) tail at the same position as cT12. cN48.1 was a 243-bp cDNA which overlapped with the 5′ end of cT12 and extended 11 bp further upstream of its 5′ end.

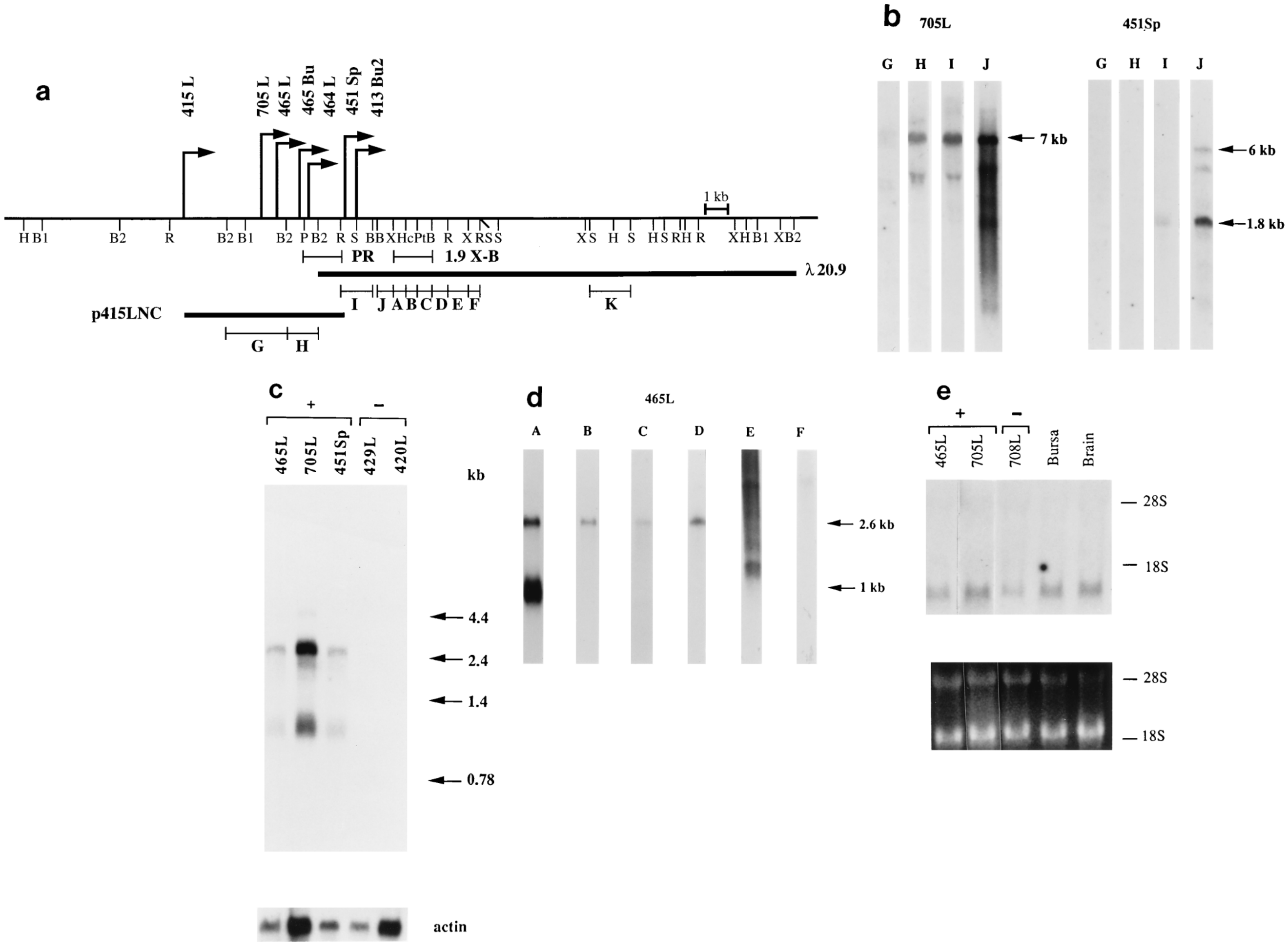

FIG. 1. Transcript analysis at the *bic* locus. (a) Restriction map of the *bic* locus. B, *Bam*HI; B1, *Bgl*I; B2, *Bgl*II; H, *Hin*dIII; Hc, *Hin*cII; P, *Pvu*II; Pt, *Pst*I; R, *Eco*RI; S, *Sac*I; X, *Xba*I. (Not all restriction sites for each enzyme are shown). Each proviral integration at the *bic* locus in independent tumors is indicated by an arrow. 415L, 464L, 465L, and 705L, metastatic lymphomas in livers from birds 415, 464, 465, and 705. 451Sp, metastatic lymphoma in spleen from bird 451. 465Bu and 413Bu2, bursal nodules from birds 465 and 413. λ20.9 was a 20.9-kb *Bgl*II genomic clone obtained by screening a chicken genomic library by using the PR (1.6-kb *Pvu*II-*Eco*RI fragment) probe. 415LNC is a 7.5-kb *Eco*RI tumor-specific junction fragment cloned from 415L tumor DNA (14). The locations of probes which detected transcripts in Northern blots (b to e) are also shown. (b) RNAs from tumors with *bic* integrations were hybridized to probe G (2.6-kb *Bgl*II-*Bgl*II), H (1.4-kb *Bgl*II-*Bgl*II), I (1.4-kb *Eco*RI-*Bam*HI), and J (0.7-kb *Bam*HI-*Xba*I). Twenty micrograms of total RNAs was used for probes G, H, and I; 1 μg of poly(A)$^+$ RNA was used for probe J. Transcripts indicated by arrows are most likely read-through transcripts that retained intron 1 (see text). The signals at about 4 kb of size (unmarked) may represent nonspecific hybridization to rRNAs. (c) Two micrograms of poly(A)$^+$ RNAs from lymphomas carrying a proviral integration at the *bic* locus (+) or lacking an insertion at *bic* (−) was hybridized to probe 1.9 X-B (1.9-kb *Xba*I-*Bam*HI). The blot was stripped and rehybridized with a chicken actin probe. (d) One microgram of poly(A)$^+$ RNA from 465L was hybridized to probes A (0.5-kb *Xba*I-*Hin*cII), B (0.4-kb *Hin*cII-*Pst*I), C (0.6-kb *Pst*I-*Bam*HI), D (0.6-kb *Bam*HI-*Eco*RI), E (0.9-kb *Eco*RI-*Xba*I), and F (0.6-kb *Xba*I-*Sac*I). The smear observed in lane E is most likely due to nonspecific hybridization of probe sequence to RNA. (e) Total RNAs (20 μg each) from tumors positive (+) or negative (−) for a proviral integration at the *bic* locus and normal adult brain and bursa were hybridized to probe K (1.8-kb *Sac*I-*Sac*I).

Since no cDNA clones isolated from the standard cDNA cloning could unambiguously represent the short 1-kb *bic* transcript, the 3′ RACE procedure (24) was employed to obtain cDNAs representing the 3′ end of the 1-kb bic_S transcript by using a *bic*-specific primer (primer A) and an oligonucleotide primer specific for the poly(A) tail. Sequencing of the resulting clones of the PCR products (cT3′R; Fig. 2) showed that they were colinear with the genomic sequence and terminated with poly(A) tails at a polyadenylation site upstream of that for cT12 and cN43.1. This result indicates that the 1-kb transcript is derived from alternative polyadenylation at a noncanonical polyadenylation signal ATTAAA (73) (see Fig. 3).

The total lengths of the cDNA sequences obtained thus far were smaller than those of the transcripts observed in Northern blots. Therefore, the structure of the 5′ ends of the transcripts was determined by 5′ RACE, which generated specific PCR products of about 560 bp (cN5′R-1; Fig. 2) and 100 bp, respectively. The smaller product was determined by Southern hybridization to nested primers to be truncated cDNAs. Since the larger product was not sufficient in quantity to be subcloned, a second nested PCR amplification was performed by using an upstream *bic*-specific primer (primer E; see Materials and Methods) to generate enough products for cloning. This primer was derived from the genomic sequence of probe J (Fig. 1a) and was shown to hybridize to the 560-bp product but not the 100-bp product. Sequencing of five of the resulting subclones (cN5′R-2) showed that they all represented spliced RNAs with the same splice sites and with the same 5′ end. The cDNA sequence upstream of the splice site was demonstrated to be genuinely derived from the *bic* locus since restriction fragments of expected sizes were detected in Southern analysis with cN5′R-2 as a probe. The remaining structure of cN5′R-1

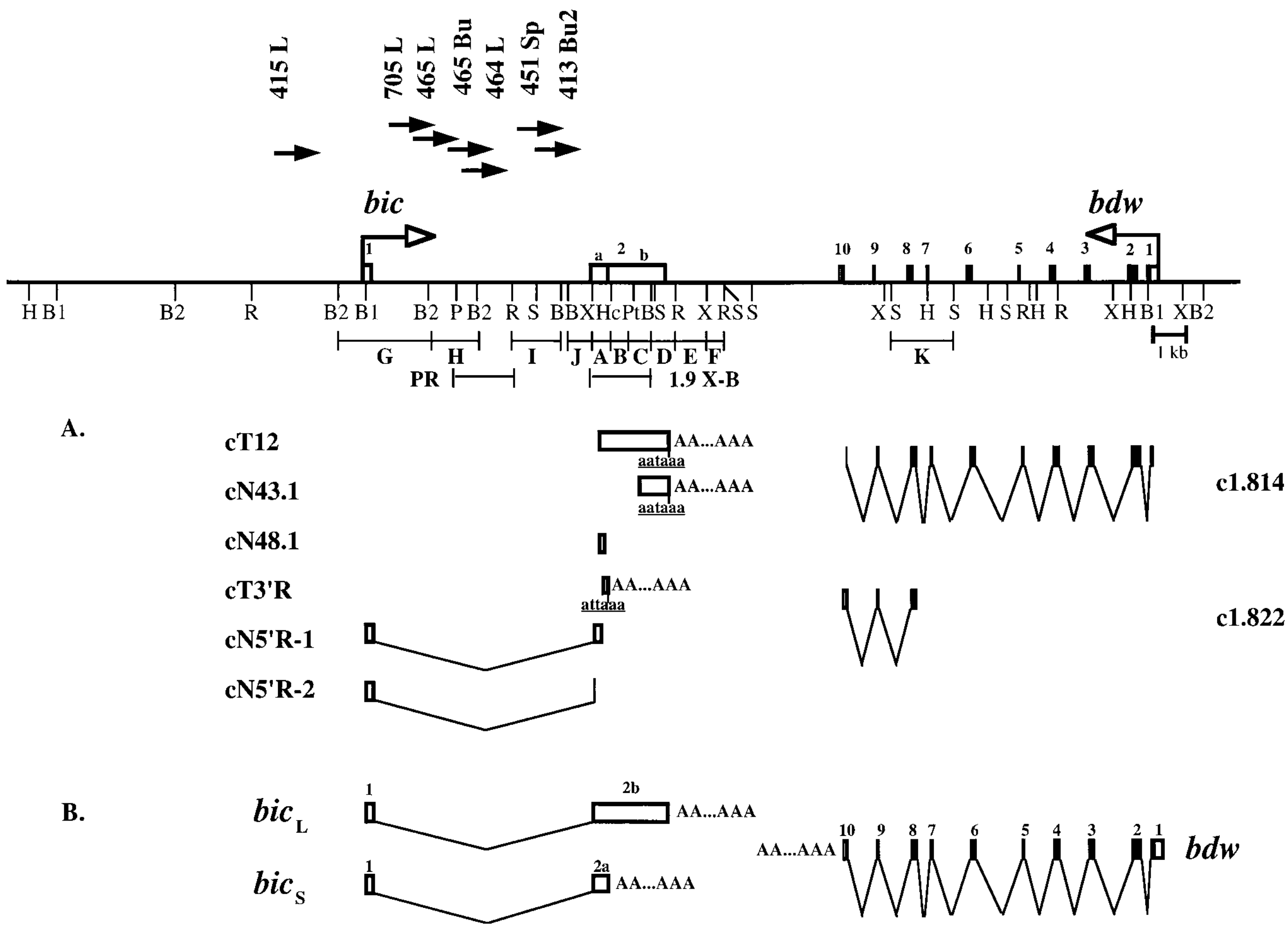

FIG. 2. Structure of the *bic* and *bdw* genes and transcripts. Boxes denote exons of the *bic* and *bdw* genes, and solid areas denote coding regions. Open arrows indicate the orientations of the two genes. Exon 2 has two alternative polyadenylation sites, resulting in a small (2a) and large (2b) second exon. (A) Representative cDNA clones from which the structures of the *bic* and *bdw* transcripts were delineated are shown. cT12, c1.814, and c1.822, cDNA clones obtained from a metastatic lymphoma (705L) library; cN43.1, a cDNA clone obtained from a normal adult chicken spleen library; cT3′R, a 3′-RACE clone obtained from lymphoma 465L; cN5′R-1 and R-2, 5′-RACE clones obtained from a normal 10-week bursa. Restriction sites are designated as in Fig. 1. (B) Deduced structures of bic_L, bic_S, and *bdw* transcripts.

was then determined by PCR with a primer upstream of the splice site (primer F) and primer D (see Materials and Methods). The use of a single splice donor and acceptor site was further confirmed by reverse transcriptase PCR (RT-PCR) with primers specific for sequences upstream and downstream of the splice site. The total sizes of the cDNA clones isolated for bic_L and bic_S transcripts were 2,436 and 780 bp, respectively. Thus, if we assume a poly(A) tract of about 200 bp, these cDNA sequences account for all, or essentially all, of the 2.6- and 1-kb transcripts identified by Northern analysis.

Structure and sequence of *bic*. Mapping and sequence analysis of the cDNA clones showed that *bic* is composed of two exons (exon 1 and exon 2) separated by an intron of about 6 kb (Fig. 2). The two splice sites (Fig. 3) conform to consensus sequences for splice donors and acceptors (61). The two *bic* transcripts are derived by alternative polyadenylation in exon 2, resulting in a small and a large exon 2 (2a and 2b, respectively). Since the more upstream polyadenylation signal is noncanonical (ATTAAA), it would result in inefficient cleavage (31). The complete cDNA sequence of *bic* is shown in Fig. 3. The genomic sequence flanking the 5′ end of the 5′ RACE clone (small letters) was obtained by sequencing the corresponding region from p415LNC (14). A potential TATA box is located 27 nucleotides upstream of the 5′ end of the 5′ RACE clones. This provides further evidence that the 5′ end of the cDNA sequence is within a few nucleotides of the 5′ end of the transcripts. Comparison of the genomic sequence with the cDNA sequence also revealed eight possible polymorphic differences.

Computer search of the database with the *bic* sequence revealed no significant homology with other known genes. Interestingly, there was no extensive ORF in the cDNA sequence (Table 1). The longest ORF in exon 2a was ORF IIIA, which was only 198 bp long. However, within this ORF, there was an allelic polymorphic insertion in the (A) stretch which would produce a frameshift in the coding sequence (see ORF IIIb): comparison of the cDNA sequence with the genomic sequence showed that while there were seven A's in the cDNA sequence, there were eight A's instead in the genomic sequence. In order to confirm that the difference in the number of A's in the (A) stretch was due to allelic polymorphism, genomic DNA isolated from normal muscle of chicken 465 was PCR amplified, and the resulting clones were sequenced (see Materials and Methods). Out of seven clones, four possessed seven A's and three had eight A's. Moreover, this polymorphism was linked to a C-T polymorphic substitution within the intron, which was located 82 bp upstream of the (A) stretch. The stretches of seven A's and eight A's were associated with the intron se-

```
-139                                                                ctctctct ctctctctct
-121   ctctcttttt tttttttaa gctctgttct aagaaaagga aagcagggga tttactcaag
 -61   acggttagtt atgagtcacc ttcatgactt ataaagggtc tcccgttgtt tggaacgggc
   1   TTTCTTCACC TAACTCGTGC TGCAGGGATA TCGGGCGACC AGCCAGACCA GCAGACCTCT
  61   GCGGCAACTG CTGATGCCTC AATGGCTTTT TTTTTCATTT TTGTTTGCCT TATTTCTCTC
 121   TCTATCTCTC TCAGAAAAAA AAAAAAAAAA GAATACAGCC CAGGCTAAGT GATCATGGTT
 181   AACATGTGAG ATGGAACAAA GGAAGTCTGT GGCCTCCTTG CTGCATTGGT TTTGCTTGCA

        [gtaggtttttcagtttggttctttggc......tttctttttctcttttttattctatag]
                                        ↓
 241   TCTCTGTGTA AAGAAACTGC CTCGTAGCAG GTATCTCAAG GGGGAAAAAA ACAGAGGTTT
 301   CAGTTCTGTA TGTCTCAGAC TCCAGTCTCT AGAGTTCTTC TGTAGGCTGT ATGTTGTTAA
 361   TGCTAATCGT GATAGGGGTT TTTACCTCTG AATGACTCCT ACATGTTAGC ATTAACACTG
 421   TACCATGCCT CTCATCAGAA CTCACAAGGA ACAAACTGCT GCTGTGGGAG GAGGACAGAA
 481   ATCATGAATC AGTCAATGCC ACGCTGAGAA GACCTCCATG TGACATGTAA AAAGATGGCT
 541   TGTTCTGCAA ACAGACGCAC TTGGTAGAAT GTGGTCTAAG TTAAGGGCAC TGGGAAAAAG
 601   CAGCTTCATG TATCAGTAAA TCCTTAGTAG GACATAGAAT CTGTAATATT CTTAGCTCAG
 661   CAACTTGGTT GTCTTCTTTT TTTCTAACTG CTTTTCAGGT CTTCTGGCTT TACTTCTTGC
 721   GTAAATGTTT CATTACATTA TTTCATTTAA GAAAGTGATT AATTAAAATT TTGGCATGCA
 781   TAAGTGTGCA TTCTTTTCTA TAATTTCATT ATATTTAAGA CAAAAACTAA CAAAAAAATG
 841   CTTCTCTGAG ATTGTAACTT TAGTTAACAC ATTTTATCGT TAAGAGAAAA TGAAAATATA
 901   TTAATTTTAC TCTGAAATTA GAGTACTTTC CAAAATTTTA CAAAAATCTC AGGATATTCC
 961   CAAGAGATAG GTAAATACTG TTATAACTGT TTTGTGGAAG GTCAAAATAG ATAGATAGTA
1021   AATACTCATA AAAATTGAGA CAGCGAGGCT TTGAAATATT TGATCTTACG CTCTAATTAA
1081   AACTGCTTAA TGAGTAGTCA TGGGCGAACA TAAGGAGAAA ATAAAGACCC AAAGGATAGA
1141   TTATTAAGTA AGAAAAGAAA CAAGGTCAAC GTCTGTGCTC TTCCAATATG TATATCCTGT
1201   CTACAGTGTT TTGACTGTGA ACCCCCAGAG TGTTTTGACT GTGAACCCCC AAGCACCTTG
1261   GTTACAGAGC ACCTTGGTTA CAGAGCACCT TGACACCACA AACACTTATG AATCAATGGC
1321   CTCATCTATA AAACAGTCTC ACATATCAAC AGTCTCACTG AATACCACTT TTCCACTCAG
1381   GTAGGACTGC TGCAGGGCAT GACTCTTCCA AAACAGGTTG TGAGATCAGA AGCTCCACTG
1441   GGAACATAAG CAATAAGAGG TTGTGCCCAC CTGAACACAA GAGCCAGCTC ACTCCTTCCA
1501   AAGTCAGAGC CAAAAAATAA AAAAAAAACA TATTTCTATT AATTTCACTG GATAATTAAC
1561   TCTGAAAGTG GGAAGGAAAT TATGGTGGGA GAGAAGAGTC AATGGAAATT CTCATTTTTT
1621   TGAGCCTAGG GTGAAATGGC ACAGCACAGC CTGATTCCAC TGCCAACTTG AGGCAAAGTT
1681   TGGAGGTATC AGTTCTCTTT GTGAAGTTGA GGTGGTCCTG AGACCCTAGA AGTGGGCAGC
1741   CATTCCCATG TTAGCAGCTC ACTGCTGTTC TTCTTCTTGG CAGCACTGTT GCCAGAGGGC
1801   TGGCAGCAGG TCCCAAGCTG CCCTGGTACA GCTGCACTAC ATGGTGGCAA AGAAGAGTCC
1861   TGGCTGAACC ATGGGCTTGG AACGTCTCTT TTAACACAAA GACTTCTGTG AAATGAAGAA
1921   AACTGAAGAT ATTATTGTGT TTATCTCTGT AAGCTAAATT CTCACATGGG TTGTACAGAT
1981   TAAAAAGGAG CATTAATTAA GTGATGATGT TTATTATATA CTCCCAAAAG GAAAATATTA
2041   CTCGATACAC TCCTTGGATC CTCACTCTAT TCAGTAAGTC TCATTTACTG TGTGGCATCA
2101   GTAAGGGATT TTTGTCTCTT CTTCAGAGCC TTAAAGCAAC AACGGAGCTC TGTACATGGC
2161   ATACACTACT GACCTCAGTG ATCATGAGTT GCATGCTACT CAAATAATGA CATCCTCATT
2221   TCACCCCATC TATTCACTCT CCAACCTGCA TTCCCCATTT CTGTCCTATA TACACTCATG
2281   GCAATAGAAG TTATGCTTCC AAGGAAGAGA ATGGGTCTCG ATTCTCACTG TCATGCTGTA
2341   AAAATCATAT GCATGTTCTC ATACATTTTC TCCCTTTAAA ATGTAAATGA AAGTGACTT
2401   GTGAACTTAA GAAATAAATA GCACATAAAA ATAAAAAAAA AAAAAAAAAA AAAAAAAAA
```

FIG. 3. Nucleotide sequence of *bic*. cDNA sequence is shown in uppercase letters and 5′ flanking sequence in lowercase letters. Position of intron is indicated by a vertical arrow, and sequence of the 5′ and 3′ ends of the intron is shown in brackets. A potential TATA box and the two polyadenylation signals are underlined. The (A) stretch within ORF III (see text) is also underlined.

quences [79 to 87 bp upstream of the (A) stretch] TTTTCT TCT and TTTTCCTCT, respectively (data not shown). This observation indicates that the difference in the number of A's in the (A) stretch is indeed due to allelic polymorphism instead of PCR artifacts. ORF III was also preceded by a very short ORF 4 nucleotides upstream of its translation initiation codon. Although reinitiation may be possible, it is not expected to be efficient because of the short intercistronic distance (36). Therefore, this ORF is not likely to function as the coding region. The two longer ORFs in exon 1 (ORFs I and II) both contain a polymorphic insertion (described above) in a long (A) stretch, which too will generate a frameshift. ORFs that are located exclusively in exon 2b are very unlikely to be relevant since they cannot be translated from the short *bic* transcript. In addition, since the chance of an ORF being translated in vivo decreases with increasing distance from the 5′ terminus of the transcript, these ORFs are not likely to be translated because of the large distance from the 5′ end of the RNA (37). This leaves three ATG ORFs longer than 45 bp that possibly code for a functional protein: ORFs V, VI, and VII. ORF V was associated with a weak Kozak initiation sequence (38). There was a pyrimidine (T) at the −3 position, despite C's at positions −1, −4, and −5. The translation initiation sites for both ORF VI and VII were in reasonable Kozak context (38) by having a purine at the −3 positions. However, none of the other positions match the optimal Kozak sequence. To assess whether any of these ORFs, as well as the other short ORFs, are likely to encode a protein product, we used the GRAIL program. It uses a neural network which combines a series of analyses to predict coding potential based on a number of parameters common to protein-coding DNA sequences (67). This program was designed for human DNA sequences, but it also works well with other organisms. GRAIL analysis predicted that none of the available ORFs are likely to encode a protein. The highest probability (0.17) was scored by a short region in exon 2b near the 3′ end of the transcript. Only regions with scores higher than 0.5 are considered to have coding potential. The longest ORF initiated from a CTG in the short *bic* transcript potentially encodes a peptide of 39 amino acids and overlaps with the longest ATG ORF. However, this ORF is in a poor context for translational initiation (TACCT CTGA) (38).

TABLE 1. ORFs larger than 45 bp initiated with an ATG in the *bic* cDNA sequence

ORF	Position[a] Start	Position[a] Stop	Frame	Amino acids	Initiator sequence
I	74	169	2	32	TGCTGATGC
II	82	165	1	28	CCTCAATGG
IIIA[b]	191	38	2	66	GTGAGATGG
IIIB[b]	191	344	2	52	GTGAGATGG
V	403	504	1	34	CCTACATGT
VI	425	484	2	20	GTACCATGC
VII	569	616	2	16	GTAGAATGT
VIII	776	880	2	35	TTGGCATGC
IV	1,100	1,144	2	15	TAGTCATGG
X	1,316	1,381	2	22	AATCAATGG
XI	1,399	1,446	1	16	AGGGCATGA
XII	1,748	1,864	2	39	TTCCCATGT
XIII	2,004	2,204	3	67	AAGTGATGA
XIV	2,156	2,284	2	43	TGTACATGG
XV	2,278	2,376	1	33	CACTCATGG

[a] The numbers refer to the nucleotide positions in the cDNA sequence (see Fig. 3).
[b] ORFs IIIA and IIIB spanned the first and second exons. The first 33 amino acids of these two ORFs were identical. Their difference in length was due to a polymorphism which resulted in a frameshift.

To examine more directly whether any of these ORFs can be translated, RNA transcripts generated in vitro from a linearized plasmid containing the full-length cDNA construct for bic_S were translated in vitro by using rabbit reticulocyte lysates. The translated products were then fractionated by using a polyacrylamide gel designed to separate proteins of low molecular weights (59). Although some protein products were synthesized, they appeared to be nonspecific because the sizes of the protein products were too large to be translated from any of the ORFs initiated with either an ATG or CTG. Moreover, these apparent products were shown not to be derived from any of the ATG ORFs longer than 45 bp within the bic_S transcript (ORFs I to VI; see Table 1) by in vitro translations of RNAs with the translation initiation codon of one of these ORFs converted to TTG by site-directed mutagenesis (data not shown).

Expression of *bic* in normal tissues. Expression of *bic* in diverse normal adult chicken tissues was examined by both Northern analysis and RNase protection assay. *bic* transcripts (2.6 and 1 kb) were detected in Northern blots (Fig. 4a) at very low levels in the bursa, thymus, and spleen. This lymphoid/hematopoietic tissue specificity of expression was confirmed by RNase protection assays using an antisense *bic* probe spanning exon 1 and exon 2 (Fig. 4b). Autoradiographic exposure for 2 weeks failed to detect any protected fragments in adult tissues other than the bursa, thymus, and spleen. Two major protected fragments (indicated by arrows) were detected. The larger protected fragment was presumably generated from protection by the spliced *bic* transcripts. It appeared to migrate slightly faster than expected, possibly because of enzymatic overdigestions at the ends of the protected fragment. The size of the smaller fragment implied the presence of a *bic* transcript that contained exon 1 but not exon 2. This transcript possibly represented an unspliced normal cellular *bic* transcript which terminated in intron 1 (see below). However, it has not yet been detected in Northern analysis. Alternatively, the smaller protected fragment may be derived from hybridization of the probe to *bic* pre-mRNAs.

To determine whether *bic* expression is developmentally regulated in lymphoid tissues, bursa, thymus, and spleen were examined for *bic* expression at different stages of development. As shown in Fig. 4c, *bic* was expressed at extremely low levels in bursas of 15- and 18-day chick embryos and in bursas of hatching chicks, but its expression became readily detectable in bursas of 1-week-old chicks and remained relatively constant as the animals matured. In the thymus and spleen, *bic* expression seemed to follow a pattern similar to that in the bursa.

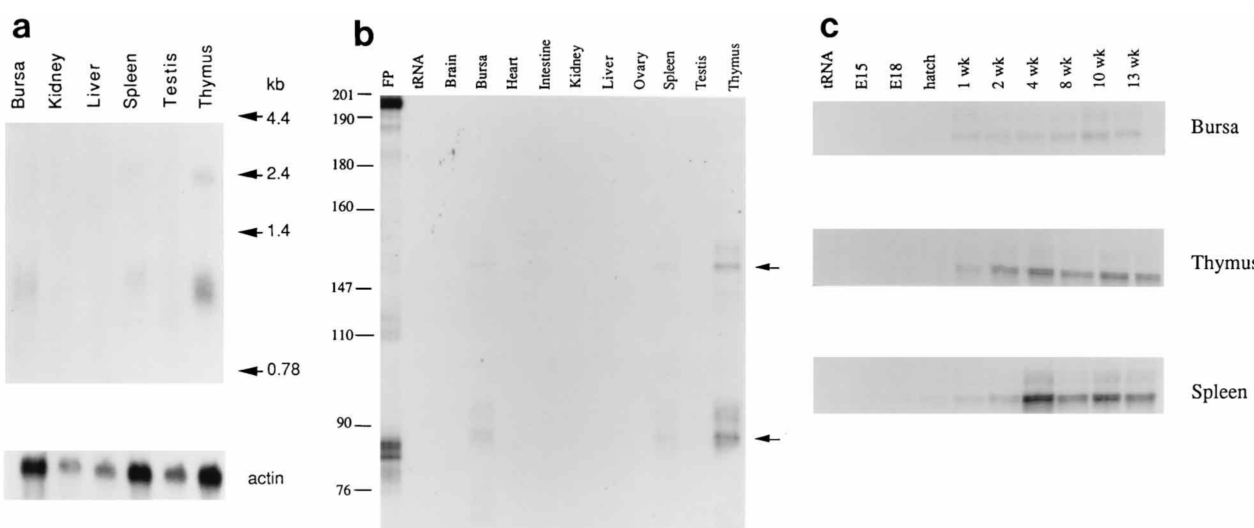

FIG. 4. Expression of *bic* in normal chicken tissues. (a) Northern blot with poly(A)$^+$ RNA from adult chicken tissues was hybridized to a *bic* cDNA (exon 1 plus exon 2a) probe. Autoradiographic exposure was for 7 days. The blot was stripped and rehybridized to a chicken actin probe. (b) Total RNAs (20 μg) isolated from a variety of chicken tissues were subjected to RNase protection analysis as described in Materials and Methods using ^{32}P-labeled antisense RNA generated from pHc-X.UE, which contains a partial cDNA insert spanning nucleotides 183 to 335 of *bic*. Yeast tRNA (20 μg) was used as a negative control. FP, undigested probe. The two major protected fragments are indicated by arrows. (c) Total RNAs (20 μg) from bursas, thymuses, and spleens of chickens at different developmental stages were subjected to RNase protection analysis as described for Fig. 4b. E15 and E18 represent 15- and 18-day embryos, respectively. Hatch is at day 21 of embryogenesis. Wk, weeks post-hatch. Only the larger protected fragments are shown in this figure.

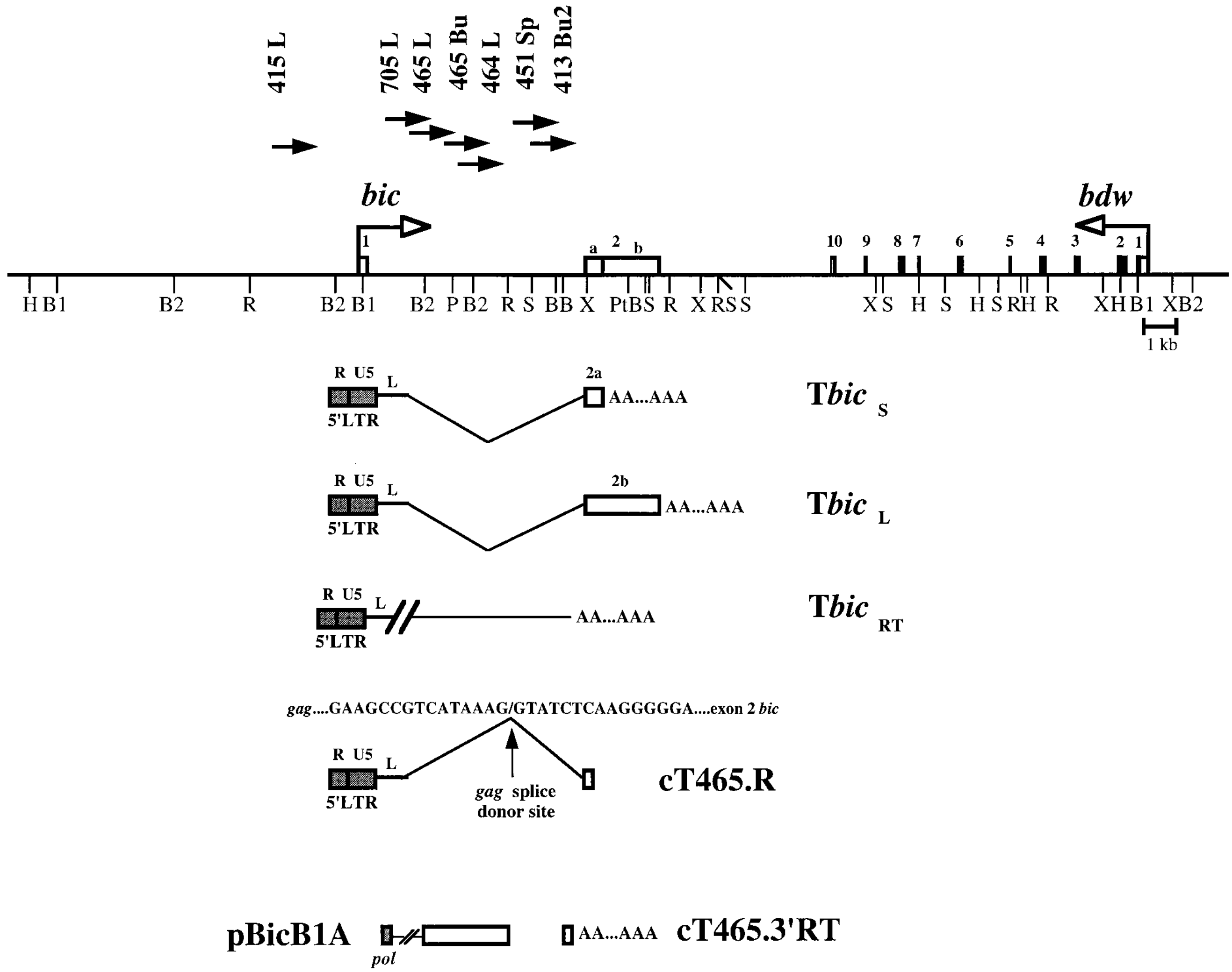

FIG. 5. Structure of chimeric transcripts in lymphoma 465L. In the tumor T*bic*$_S$ and T*bic*$_L$ transcripts, the 5′LTR of the provirus was covalently linked to *bic* exon 2 through a splicing event using the *gag* splice donor and the *bic* exon 2 splice acceptor. T*bic*$_{RT}$s were unspliced read-through transcripts initiated from the 5′LTR and contained viral sequences linked to intron 1 sequences. cT465.R, a cDNA clone derived by PCR amplification of reverse-transcribed 465L RNA using a U5-specific primer and a *bic* exon 2 primer. The sequence of the virus-*bic* junction is indicated. T465.3′RT, a 3′ RACE clone obtained from 465L which represents the 3′ end of the read-through transcripts. pBic.B1A, a partial cDNA of a read-through transcript (14).

Activation of *bic* expression by promoter insertion. All of the proviral integrations mapped within the *bic* intron, except for that in 415L which is 5′ of exon 1. Since all the proviral integrations were in the same transcriptional orientation as *bic*, it seemed likely that *bic* is activated by a promoter insertion mechanism. To determine whether this was indeed the case, RT-PCR was performed on RNA isolated from 465L with a viral U5 primer and a *bic* exon 2a-specific primer. Specific PCR products were cloned and sequenced. Sequence analysis of the resulting subclones showed covalent linkage of the U5-leader-*gag* sequence of RAV-2 with exon 2 through a splicing event between the *gag* splice donor and the exon 2 splice acceptor (cT465.R; Fig. 5), indicating that the integrated provirus activates *bic* expression by promoter insertion. These chimeric transcripts in the tumors and the normal *bic* transcripts appeared similar in size in Northern blots because exon 1 of *bic* (270 bp) was replaced by the viral LTR R-U5-leader-*gag* sequences (approximately 400 bp).

The tumor-specific transcripts shown in the Northern blots of Fig. 1b (probes G to J) were most likely read-through transcripts which were initiated from the viral promoter and read into intron 1 (T*bic*$_{RT}$; Fig. 5). This was further supported by the structure of the partial cDNA clone pBicB1A, which contains *pol* sequences and intron 1 sequences at its termini (14). Based on Northern analysis, these transcripts appeared to terminate within the 0.7-kb *Bam*HI-*Xba*I genomic fragment (probe J; Fig. 1b). We wanted to characterize these transcripts further by obtaining cDNAs for their 3′ ends. 3′ RACE was employed for this purpose with a primer within the 0.7-kb *Bam*HI-*Xba*I fragment (primer B) and an oligo(dT) primer. Two of the resulting clones (cT465.3′RT) were sequenced and shown to be colinear with the genomic sequence and to contain poly(A) tails (Fig. 5). These two clones were identical except that they had different poly(A) sites, which differed in position by only 2 nucleotides. There was a canonical (AATAAA) polyadenylation signal 22 to 24 nucleotides upstream of these poly(A) sites, indicating that the 3′ ends of these clones genuinely represent the 3′ end of read-through transcripts (data not shown). From these results, we determined that some read-through transcripts terminated upstream of exon 2, 228 or

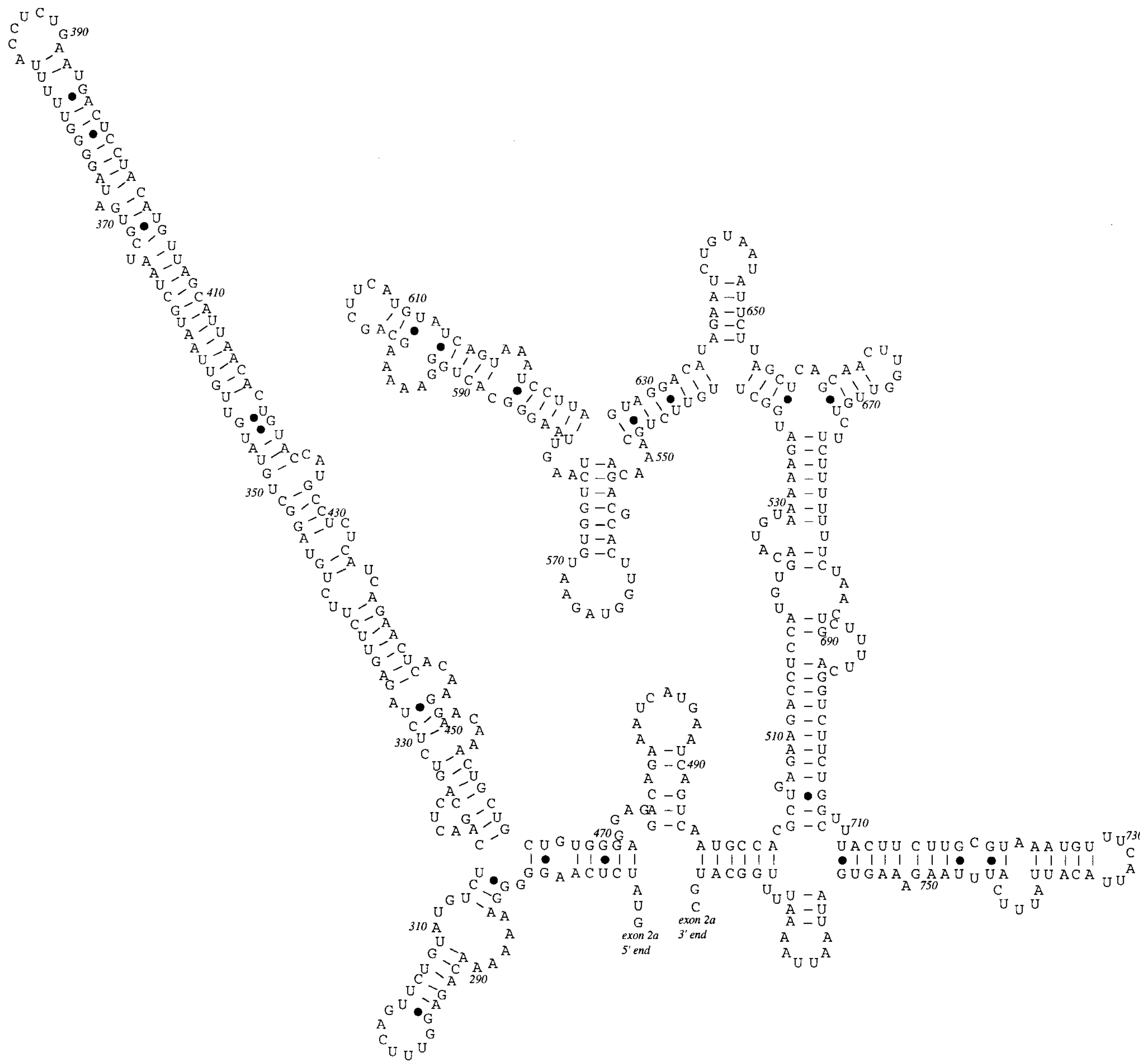

FIG. 6. Computer-generated RNA secondary structure of *bic* exon 2a. RNA secondary structure of *bic* exon 2a was predicted by using the FOLDRNA program. The nucleotide positions within *bic* exon 2a are indicated.

230 nucleotides downstream of the *Bam*HI site of the 0.7-kb *Bam*HI-*Xba*I fragment (probe J).

***bic* exon 2a is predicted to form extensive secondary structures.** The absence of an extensive ORF suggests that *bic* functions through its RNA. Since a noncoding RNA is likely to function by virtue of its secondary structure, we attempted to determine the RNA secondary structure of *bic* exon 2a by using the base-stacking energy method of Zuker and Stiegler (74). *bic* exon 2a was chosen for secondary structure analysis since this region was present in both tumor and normal bic_S and bic_L transcripts and hence would most likely mediate the biological activity of *bic*. As shown in Fig. 6, *bic* exon 2a RNA was predicted to form extensive secondary structures. In particular, the region between nucleotides 316 and 461 had the potential to form a highly ordered and energetically favorable stem structure. The potential for *bic* exon 2a RNA to form substantial secondary structures provides further support that *bic* indeed functions through its untranslated RNA.

Sequence, structure, and expression of *bdw*, a gene downstream of *bic*. The 1.8-kb *Sac*I genomic fragment (probe K) identified a 1.4-kb transcript, and the gene from which the transcript was derived was designated *bdw* (*bic* downstream). cDNAs for this gene were isolated from a library derived from tumor 705L. From the sequences of two overlapping cDNA clones, c1.814 and c1.822 (Fig. 3), and a genomic sequence flanking the 5′ end of c1.814 and the 3′ end of c1.822, the complete nucleotide sequence of the 1.4-kb transcript was determined (Fig. 7). It encoded a putative novel protein of 345 amino acids. Comparison of the cDNA sequence with the genomic sequence from a normal chicken revealed a base

```
                                                          60                                                           120
ccctgtaaacacagcacagttgtttcaatctgtcccacaagatccacaatcatccgcgtaggggcagtgtaacctcctggtataagaacacgtgtggactgcagaggagggctgaacgcc
                                                         180                                                           240
ggagccttgctaacacagcacagatggactaaaacgaatccagagggtccacgacagacgaggtctcacggagccagcctggcggcagatagcggagcggcggggaaccatgctgccgc
                                                         300                                                   ↓       360
tgccgttgtttccaggggagcctggcggagaatgcacaggggctgaattggagcATGGCGGCGTGCTGGGCCGCCCGCTGCCTGCGGGGCAGGCGGGAATGGCGCAGGTTCAACTCTACA
                                                        M  A  A  C  W  A  A  R  C  L  R  G  R  R  E  W  R  R  F  N  S  T

                                                         420                                                           480
CTCTCTGCTTCTCGACTGACATCAGATGAAGTTATTCGGATGCGTAATGAACTCTTTACCAAAGAGAAGGAGAGGCAGTTATCTCTTTATCCACGAATTGAGAAAATTGAAGTGAAATAC
 L  S  A  S  R  L  T  S  D  E  V  I  R  M  R  N  E  L  F  T  K  E  K  E  R  Q  L  S  L  Y  P  R  I  E  K  I  E  V  K  Y
                                                         540          ↓                                                600
ATGGGAAAATCTCACCCTGGCAGTGTGTTTGTAATGAACAAAGCTTTGTCTACGCCATACAATTGTGCCATGCATTTAAGCGAATGGCATTGCAAGAAATCTGTTCTAGCTCTTGTGGAT
 M  G  K  S  H  P  G  S  V  F  V  M  N  K  A  L  S  T  P  Y  N  C  A  M  H  L  S  E  W  H  C  K  K  S  V  L  A  L  V  D
                                                         660                             ↓                             720
GGTGAAGTCTGGGATATGTATAGACCCTTGACCAAGTCTTGTGAAATTCAGTTCCTCACCTTCAAAGATGAAGATCCAGAGGAAGTAAACAAGGCCTATTGGCGTTCCTGTGCCATGATC
 G  E  V  W  D  M  Y  R  P  L  T  K  S  C  E  I  Q  F  L  T  F  K  D  E  D  P  E  E  V  N  K  A  Y  W  R  S  C  A  M  I
                                                         780     ↓                                                     840
ATGGCAAATGTGCTAAAGCGGGCATTCAAAGATGAGTACTCTGTGACTCTGGTTAAATCTCCAGAAGTGCCAGTGATCTCTGGAGCTTTCTGTTATGATGTAATTTTGGACAATAGACTG
 M  A  N  V  L  K  R  A  F  K  D  E  Y  S  V  T  L  V  K  S  P  E  V  P  V  I  S  G  A  F  C  Y  D  V  I  L  D  N  R  L
                    ↓                                    900                                                           960
AATGACTGGAAACCAGCAAAAGACAACTTCCGTTCTCTTACAAGGGATGCCAATAAGCTAATTGATAAAGACCTGCCATTTGAAACACTGCATGTTGAAGCAAAAGTGGCGCGTGAAATG
 N  D  W  K  P  A  K  D  N  F  R  S  L  T  R  D  A  N  K  L  I  D  K  D  L  P  F  E  T  L  H  V  E  A  K  V  A  R  E  M
              ↓                                         1020                        ↓                                 1080
TTTCAGCATAACAAGTATAAAATGGAGCTAATAGAGCAGAAAGCTTCTCAGAACATGGAAGGAATTGTAGTATTACATAGGTTTGGTGACTTTGTCGATGTTAGTGAAGGACCTCACATT
 F  Q  H  N  K  Y  K  M  E  L  I  E  Q  K  A  S  Q  N  M  E  G  I  V  V  L  H  R  F  G  D  F  V  D  V  S  E  G  P  H  I
                                                        1140                                                     ↓    1200
CCAAGGACAAGTTTCTGTTTCCAGTATGAGATAACAGCAGCCCACATTCTTCAGACAAGTCAATCTGAATTGATAAGGAGGTTCCAGGGCGTGTCCCTGCCAATCCATTTGAGGGCTCAT
 P  R  T  S  F  C  F  Q  Y  E  I  T  A  A  H  I  L  Q  T  S  Q  S  E  L  I  R  R  F  Q  G  V  S  L  P  I  H  L  R  A  H
                                         ↓              1260                                                          1320
CACACTGTGTGGCACAAACTGCTGGAAAGATCAAAGAAACTGGTCACTCAGGAAAAAAGTATGGAAGCAGCAGCAGAAAGTCAAGAGGCAAAAGATGAAACTGAAGAAGGAAAAACTCTA
 H  T  V  W  H  K  L  L  E  R  S  K  K  L  V  T  Q  E  K  S  M  E  A  A  A  E  S  Q  E  A  K  D  E  T  E  E  G  K  T  L
TCAATGTAATTTAACCTCTAAATGTACATAAATaaaatag
 S  M
```

FIG. 7. DNA sequence and predicted polypeptide sequence of *bdw*. Nucleotide sequence derived from cDNA clones is shown in capitals. The genomic sequence flanking the 5′ and 3′ ends of the cDNA sequence is indicated in lowercase. The positions of introns are indicated by arrows. The start point of transcription is not known. The consensus polyadenylation signal, as well as a potential TATA box and putative CAAT box, are underlined. The base polymorphism (position 1290) is shown in boldface type.

difference in the coding sequence of *bdw* (Fig. 7). This would result in an Ala-to-Val substitution. This base change was confirmed to be a polymorphism rather than a somatic mutation by PCR amplification of normal tissue DNA from animal 705 (from which the tumor cDNA library was derived) by using primers flanking the base changes and sequencing the resulting clones (data not shown).

bdw consists of 10 exons, with a transcriptional orientation opposite to that of *bic*. Examination of the intron-exon boundaries showed consensus splice site sequences (data not shown). *bdw* transcript was evident in a variety of adult chicken tissues. The highest levels of expression were in the testis, brain, bursa, and kidney (data not shown). *bdw* expression did not appear to be altered by proviral integrations: the abundance and size of the *bdw* transcripts in tumors with *bic* integrations were similar to those in tumors without *bic* integrations and in normal adult bursa (Fig. 1e). The transcriptional orientation of *bdw* relative to the proviral integrations was not consistent with activation of the gene by either promoter insertion or enhancer insertion (69). These observations argue against *bdw* being the relevant gene at the *bic* locus.

DISCUSSION

We have identified two novel genes, *bic* and *bdw*, at the *bic* locus. *bdw* lies downstream of *bic* and in the opposite transcriptional orientation. While the expression of *bdw* does not appear to be quantitatively or qualitatively altered by the proviral integrations, *bic* is apparently activated by a promoter insertion mechanism, resulting in overexpression of a chimeric virus-*bic* exon 2 RNA. The activation of *bic* by proviral integrations at a common retroviral integration site in independent B-cell lymphomas strongly implies the involvement of *bic* in lymphomagenesis.

Normal *bic* appears to be expressed specifically in the bursa, thymus, and spleen. Moreover, expression of *bic* in these lymphoid/hematopoietic tissues is developmentally regulated. These observations suggest that *bic* is involved in normal cell growth and/or differentiation of B and T cells and possibly cells of the erythroid lineage. RNase protection analysis did not detect expression of normal *bic* transcripts in metastatic lymphomas 465L and 705L (data not shown). This implies that *bic* is normally silent in the bursal target cells transformed by c-*myc*. Elevated and/or inappropriate expression of *bic* caused by viral promoter insertion may then contribute to lymphomagenesis.

As proviral integrations in the *bic* locus are usually found in conjunction with *myc* activations, *bic* appears to be a collaborator of *myc*. Activation of *bic* appears to play a role in late stages of tumor progression, possibly metastasis, in avian lymphoid leukosis, since proviral integrations at the *bic* locus are found much more frequently in metastatic tumors than in primary tumors (14). It is conceivable that *bic* may contribute to metastasis in ALV-induced lymphomas by providing the bursal tumor cells the ability to grow outside the bursal microenvironment, possibly through inhibition of apoptosis (50). Further experiments are required to investigate this possibility.

An interesting feature of *bic* is that it lacks an extensive ORF, despite the fact that *bic* transcripts are both spliced and polyadenylated. There is a remote possibility that RNA editing or ribosomal frameshifting (21) may lengthen the ORF to be translated in vivo. However, because of the high density of stop codons in all three reading frames, extensive RNA editing or multiple ribosomal frameshifts would be required to substantially lengthen the ORF. The lack of an extensive ORF in *bic* raises the possibility that it is a nonfunctional pseudogene. However, *bic* cannot be a processed pseudogene because of the presence of an intron and the lack of direct repeats at the 5′ and 3′ ends. Although we failed to demonstrate evolutionary conservation of *bic* in zoo blots using DNAs from *Drosophila*, mouse, and human, Southern analysis under low stringency conditions did not detect any related sequences of *bic* in chickens (data not shown). Most importantly, the expression of *bic* is tissue specific and developmentally regulated, demonstrating a delicate control for *bic* expression. Therefore, it is highly unlikely that *bic* is an unprocessed pseudogene.

Available data from the characterization of two mammalian genes, *H19* and *Xist*, provide support that *bic* may function through its RNA. Both of these genes share with *bic* the special feature of having no extensive ORFs. Comparison of the sequences of the mouse and human homologs of each of these genes demonstrated that, despite the extensive conservation throughout the entire gene, none of the small ORFs are conserved between these two species (7–9), implying that neither of these genes is likely to encode a functional protein. Moreover, the localization of transcripts of these two genes is incompatible with their being translated. Cell fractionation studies showed that *H19* is not associated with polysomes in the cytoplasm (7). Fluorescence in situ hybridization and cell fractionation studies also demonstrated localization of *Xist* RNAs within the nucleus (8, 9). This lack of association with the translational machinery of the cell strongly suggests that *H19* and *Xist* produce functional untranslated RNAs.

There is growing evidence that untranslated RNAs can have important biological functions. Ectopic expression of the *H19* gene resulted in prenatal lethality (10), suggesting that *H19* may play a role in mammalian development. The *Xist* RNA is involved in X-chromosome inactivation (8, 9, 32, 44, 52, 54, 57, 58), possibly as a component in a nonchromatin nuclear structure that associates specifically with the inactive X chromosome (13). Moreover, recent data have emerged which showed that untranslated RNAs can play a role in cell growth and differentiation, as well as transformation and oncogenesis. The human *H19* gene, when transfected into embryonal tumor lines, caused growth inhibition and morphological changes. Moreover, clonogenicity in soft agar and tumorigenicity in nude mice were abrogated in one of the transfectants (25), indicating that *H19* can function as a tumor suppressor. Disruption of normal imprinting of the *H19* gene may contribute to tumorigenesis (18, 30, 33, 65, 68). Furthermore, genetic complementation studies revealed the ability of the 3′ untranslated regions (3′ UTR) of α-actin, tropomyosin, and troponin I to partially complement the mutant phenotype of a nondifferentiating myogenic cell line, NMU2. These UTRs, particularly the 3′ UTR of tropomyosin, are capable of promoting expression of differentiation-specific genes in myogenic cell lines (55). The 3′ UTR of tropomyosin can also function as a tumor suppressor (56). Constitutive expression of a 0.2-kb RNA from the 3′ UTR of tropomyosin suppressed anchorage-independent growth and tumor formation by NMU2 cells. The recent isolation of a novel gene, *His-1*, from a common retroviral insertion site in murine leukemia virus-induced myeloid leukemia (5) gives further support that untranslated RNAs can control cell growth. The isolation of *bic* provides yet another example of the possible involvement of untranslated RNAs in oncogenesis. Importantly, this is also the first time that an untranslated RNA has been implicated in the pathogenesis of lymphomas.

Very recently, it has been demonstrated that the 3′ UTR of human α-tropomyosin RNA can activate the double-stranded RNA-dependent protein kinase PKR to inhibit translation in vitro (17), suggesting that its tumor suppressor activity may be mediated through PKR. There is growing evidence that PKR plays a role in normal cell growth and/or differentiation (35, 46), possibly by regulating gene transcription (34, 39) and/or inhibiting translation (43, 53). Double-stranded RNAs have been demonstrated to bind and regulate the activity of PKR (12, 43). Interestingly, the computer-predicted secondary structure of *bic* exon 2a RNA was notable for its double-stranded regions, which included an extended highly ordered duplex stem structure. This observation, together with the possible role of PKR in cell growth and/or differentiation and the discovery of in vitro activation of PKR by the 3′ UTR of α-tropomyosin RNA, raise the possibility that the potential biological function(s) of *bic* is mediated through PKR. Further experiments are necessary to test this hypothesis.

The identification of *bic* as a target for insertional mutagenesis in avian B-cell lymphomas strongly suggests that *bic* is involved in lymphomagenesis. Studies on *H19* and the 3′ UTR of tropomyosin have shown that noncoding RNAs can act as tumor suppressors. The data presented here, as well as the discovery of *His*-1, make it likely that untranslated RNAs can contribute to oncogenesis. Moreover, our studies suggest that atypical RNAs like *bic* may represent a novel class of *myc* collaborators. Nevertheless, we cannot completely rule out the possibility that *bic* may encode a small peptide. For instance, the *Drosophila* heat shock gene, *hsrw*, has been proposed to encode a protein of only 27 amino acids (23). We have attempted to demonstrate directly the transforming potential of *bic* and its possible oncogenic cooperation with *myc*, both in vitro and in vivo, by using retroviral vectors to express *bic* (with or without c-*myc*) in cultured cells and in animals. Collaboration between c-*myc* and *bic* in oncogenesis is evident in these experiments. In vitro, *bic* enhanced growth and morphological transformation of chicken embryo fibroblasts constitutively expressing c-*myc*. Most importantly, chicken oncogenicity assays showed that while *bic* does not appear to be oncogenic by itself, it can cooperate with c-*myc* in lymphomagenesis and erythroleukemogenesis (64). We are also trying to use these biological assays to further characterize the biological product of *bic*.

ACKNOWLEDGMENTS

We are grateful to Peter Besmer and Bruce Clurman for their critical comments and valuable discussions. We also thank Kenya Parks and MaryAnne Carroll for technical assistance.

This work was supported by NIH grant CA-16599 to W.S.H. W.T. is supported by a fellowship from the Tri-Institutional M.D.-Ph.D. Program.

REFERENCES

1. **Adams, J. M., and S. Cory.** 1992. Oncogene co-operation in leukaemogenesis. Cancer Surv. **15:**119–141.
2. **Adams, J. M., A. W. Harris, C. A. Pinkert, L. M. Corcoran, W. S. Alexander, R. D. Palmiter, and R. L. Brinster.** 1985. The c-*myc* oncogene driven by immunoglobulin enhancers induces lymphoid malignancy in transgenic mice. Nature (London) **318:**533–538.
3. **Alexander, W. S., O. Bernard, S. Cory, and J. M. Adams.** 1989. Lymphomagenesis in Eμ-*myc* transgenic mice can involve *ras* mutations. Oncogene **4:**575–581.
4. **Altschul, S. F., W. Gish, W. Miller, E. W. Myers, and D. J. Lipman.** 1990. Basic local alignment search tool. J. Mol. Biol. **215:**403–410.
5. **Askew, D. S., J. Li, and J. N. Ihle.** 1994. Retroviral insertions in the murine *His-1* locus activate the expression of a novel RNA that lacks an extensive open reading frame. Mol. Cell. Biol. **14:**1743–1751.
6. **Baba, T. W., and E. H. Humphries.** 1985. Formation of a transformed follicle is necessary but not sufficient for development of an avian leukosis virus-induced lymphoma. Proc. Natl. Acad. Sci. USA **82:**213–216.
7. **Brannan, C. I., E. C. Dees, R. S. Ingram, and S. M. Tilghman.** 1990. The product of the *H19* gene may function as an RNA. Mol. Cell. Biol. **10:**28–36.
8. **Brockdorff, N., A. Ashworth, G. F. Kay, V. M. McCabe, D. P. Norris, P. J.**

Cooper, S. Swift, and S. Rastan. 1992. The product of the mouse *Xist* gene is a 15 kb inactive X-specific transcript containing no conserved ORF and located in the nucleus. Cell **71:**515–526.
9. **Brown, C. J., B. D. Hendrich, J. L. Rupert, R. G. Lafreniere, Y. Xing, J. Lawrence, and H. F. Willard.** 1992. The human XIST gene: analysis of a 17 kb inactive X-specific RNA that contains conserved repeats and is highly localized within the nucleus. Cell **71:**527–542.
10. **Brunkow, M. E., and S. M. Tilghman.** 1991. Ectopic expression of the *H19* gene in mice causes prenatal lethality. Genes Dev. **5:**1093–1101.
11. **Chomczynski, P., and N. Sacchi.** 1987. Single-step method of RNA isolation by acid guanidinium thiocyanate-phenol-chloroform extraction. Anal. Biochem. **162:**156–159.
12. **Clemens, M. J., K. G. Laing, I. W. Jeffrey, A. Schofield, T. V. Sharp, A. Elia, V. Matys, M. C. James, and V. J. Tilleray.** 1994. Regulation of the interferon-inducible eIF-2 alpha protein kinase by small RNAs. Biochimie (Paris) **76:**770–778.
13. **Clemson, C. M., J. A. McNeil, H. F. Willard, and J. B. Lawrence.** 1996. XIST RNA paints the inactive X chromosome at interphase—evidence for a novel RNA involved in nuclear chromosome structure. J. Cell Biol. **132:**259–275.
14. **Clurman, B. E., and W. S. Hayward.** 1989. Multiple proto-oncogene activations in avian leukosis virus-induced lymphomas: evidence for stage-specific events. Mol. Cell. Biol. **9:**2657–2664.
15. **Cooper, M. D., L. N. Payne, P. B. Dent, B. R. Burmester, and R. A. Good.** 1968. Pathogenesis of avian lymphoid leukosis. I. Histogenesis. J. Natl. Cancer Inst. **41:**373–378.
16. **Cory, S., and J. M. Adams.** 1988. Transgenic mice and oncogenesis. Annu. Rev. Immunol. **6:**25–48.
17. **Davis, S., and J. C. Watson.** 1996. *In vitro* activation of the interferon-induced, double-stranded RNA-dependent protein kinase PKR by RNA from the 3′ untranslated regions of human alpha-tropomyosin. Proc. Natl. Acad. Sci. USA **93:**508–513.
18. **Doucrasy, S., M. Barrois, S. Fogel, J. C. Ahomadegbe, D. Stehelin, J. Coll, and G. Riou.** 1996. High incidence of loss of heterozygosity and abnormal imprinting of *H19* and *Igf2* genes in invasive cervical carcinomas—uncoupling of *H19* and *Igf2* expression and biallelic hypomethylation of *H19*. Oncogene **12:**423–430.
19. **Edwards, J. B., J. Delort, and J. Mallet.** 1991. Oligo-deoxyribonucleotide ligation to single-stranded cDNAs: a new tool for cloning 5′ ends of mRNAs and for constructing cDNA libraries by *in vitro* amplification. Nucleic Acids Res. **19:**5227–5232.
20. **Ewert, D. L., and G. F. de Boer.** 1988. Avian lymphoid leukosis: mechanisms of lymphomagenesis. Adv. Vet. Sci. Comp. Med. **32:**37–55.
21. **Farabaugh, P. J.** 1991. Alternative readings of the genetic code. Cell **74:**591–596.
22. **Feinberg, A. P., and B. Vogelstein.** 1983. A technique for radiolabeling DNA restriction endonuclease fragments to high specific activity. Anal. Biochem. **132:**6–13.
23. **Fini, M. E., W. G. Bendena, and M. L. Pardue.** 1989. Unusual behaviour of the cytoplasmic transcript of *hsrw*: an abundant, stress-inducible RNA that is translated but yields no detectable protein product. J. Cell. Biol. **6:**2045–2057.
24. **Frohman, M. A., M. K. Dush, and G. R. Martin.** 1988. Rapid production of full-length cDNAs from rare transcripts: amplification using a single gene-specific oligonucleotide primer. Proc. Natl. Acad. Sci. USA **85:**8998–9002.
25. **Hao, Y., T. Crenshaw, T. Moulton, E. Newcomb, and B. Tycko.** 1993. Tumor-suppressor activity of *H19* RNA. Nature (London) **365:**764–767.
26. **Haupt, Y., W. S. Alexander, G. Barri, S. P. Klinken, and J. M. Adams.** 1991. Novel zinc finger gene implicated as *myc* collaborator by retrovirally accelerated lymphomagenesis in Eμ-*myc* transgenic mice. Cell **65:**753–763.
27. **Haupt, Y., M. L. Bath, A. W. Harris, and J. M. Adams.** 1993. *bmi-1* transgene induces lymphomas and collaborates with *myc* in tumorigenesis. Oncogene **8:**3161–3164.
28. **Haupt, Y., A. W. Harris, and J. M. Adams.** 1993. Moloney murine induction of T-cell lymphomas in a plasmacytomagenic strain of Eμ-v-*abl* transgenic mice. Int. J. Cancer **55:**623–629.
29. **Hayward, W. S., B. G. Neel, and S. M. Astrin.** 1981. Activation of a cellular *onc* gene by promoter insertion in ALV-induced lymphoid leukosis. Nature (London) **290:**475–480.
30. **Hibi, K., H. Nakamura, A. Hirai, Y. Fujikake, Y. Kasai, S. Akiyama, K. Ito, and H. Takagi.** 1996. Loss of *H19* imprinting in esophageal cancer. Cancer Res. **56:**480–482.
31. **Humphrey, T., and N. J. Proudfoot.** 1988. A beginning to the biochemistry of polyadenylation. Trends. Genet. **4:**243–245.
32. **Kay, G. F., G. D. Penny, D. Patel, A. Ashworth, N. Brockdorff, and S. Rastan.** 1993. Expression of *Xist* during mouse development suggests a role in the initiation of X chromosome inactivation. Cell **72:**171–182.
33. **Kondo, M., H. Suzuki, R. Ueda, H. Osada, K. Takagi, T. Takahashi, and T. Takahashi.** 1995. Frequent loss of imprinting of the *H19* gene is often associated with its overexpression in human lung cancers. Oncogene **10:** 1193–1198.
34. **Koromilas, A. E., C. Cantin, A. W. Craig, R. Jagus, J. Hiscott, and N. Sonenberg.** 1995. The interferon-inducible protein kinase PKR modulates the transcriptional activation of immunoglobulin κ gene. J. Biol. Chem. **270:**25426–25434.
35. **Koromilas, A. E., S. Roy, G. N. Barber, M. G. Katze, and N. Sonenberg.** 1992. Malignant transformation by a mutant of the IFN-inducible dsRNA-dependent protein kinase. Science **257:**1685–1689.
36. **Kozak, M.** 1987. Effects of intercistronic length on the efficiency of reinitiation by eucaryotic ribosomes. Mol. Cell. Biol. **7:**3438–3445.
37. **Kozak, M.** 1989. The scanning model for translation: an update. J. Cell Biol. **108:**229–241.
38. **Kozak, M.** 1991. Structural features in eukaryotic mRNAs that modulate the initiation of translation. J. Biol. Chem. **266:**19867–19870.
39. **Kumar, A., J. Haque, J. Lacoste, J. Hiscott, and B. R. G. Williams.** 1994. Double-stranded RNA-dependent protein kinase activates transcription factor NF-κB by phosphorylating IκB. Proc. Natl. Acad. Sci. USA **91:**6288–6292.
40. **Langdon, W. Y., A. W. Harris, and S. Cory.** 1989. Acceleration of B-lymphoid tumorigenesis in Eμ-*myc* transgenic mice by v-H-*ras* and v-*raf* but not v-*abl*. Oncogene Res. **4:**253–258.
41. **Largaespada, D. A., D. A. Kaehler, H. Mishak, E. Weissinger, M. Potter, J. F. Mushinski, and R. Risser.** 1992. A retrovirus that expresses v-*abl* and c-*myc* oncogenes rapidly induces plasmacytomas. Oncogene **7:**811–819.
42. **Maniatis, T., E. F. Fritsch, and J. Sambrook.** 1989. Molecular cloning: a laboratory manual, 2nd ed. Cold Spring Harbor Laboratory Press, Cold Spring Harbor, N.Y.
43. **Mathews, M. B.** 1993. Viral evasion of cellular defense mechanisms: regulation of the protein kinase DAI by RNA effectors. Semin. Virol. **4:**247–257.
44. **McCarrey, J. R., and D. D. Dilworth.** 1992. Expression of *Xist* in mouse germ cells correlates with X-chromosome inactivation. Nat. Genet. **2:**200–203.
45. **McDonnell, T. J., and S. J. Korsmeyer.** 1991. Progression from lymphoid hyperplasia to high-grade malignant lymphoma in mice transgenic for the t(14;18). Nature (London) **349:**254–256.
46. **Meurs, E. F., J. Galabru, G. N. Barber, M. G. Katze, and A. G. Hovanessian.** 1993. Tumor suppressor function of the interferon-induced double-stranded RNA-activated protein kinase. Proc. Natl. Acad. Sci. USA **90:**232–236.
47. **Neiman, P., C. Wolf, P. J. Enrietto, and G. M. Cooper.** 1985. A retroviral *myc* gene induces preneoplastic transformation of lymphocytes in a bursal transplantation assay. Proc. Natl. Acad. Sci. USA **82:**222–226.
48. **Neiman, P. E.** 1994. Retrovirus-induced B cell neoplasia in the bursa of Fabricius. Adv. Immunol. **56:**467–484.
49. **Neiman, P. E., L. Jordan, R. A. Weiss, and L. N. Payne.** 1980. Malignant lymphoma of the bursa of Fabricius: analysis of early transformation, p. 519–528. *In* M. Essex, G. Todaro, and H. zur Hausen (ed.), Viruses in naturally occurring cancers, book A. Cold Spring Harbor Laboratory, Cold Spring Harbor, N.Y.
50. **Neiman, P. E., S. J. Thomas, and G. Loring.** 1991. Induction of apoptosis during normal and neoplastic B-cell development in the bursa of Fabricius. Proc. Natl. Acad. Sci. USA **88:**5857–5861.
51. **Pearson, W. R., and D. J. Lipman.** 1988. Improved tools for biological sequence comparison. Proc. Natl. Acad. Sci. USA **85:**2444–2448.
52. **Penny, G. D., G. F. Kay, S. A. Sheardown, S. Rastan, and N. Brockdorff.** 1996. Requirement for *Xist* in X chromosome inactivation. Nature (London) **379:**131–137.
53. **Proud, C. G.** 1995. PKR: a new name and new roles. Trends Biochem. Sci. **20:**241–246.
54. **Rastan, S.** 1994. X chromosome inactivation and the *Xist* gene. Curr. Opin. Genet. Dev. **4:**292–297.
55. **Rastinejad, F., and H. M. Blau.** 1993. Genetic complementation reveals a novel regulatory role for 3′ untranslated regions in growth and differentiation. Cell **72:**903–917.
56. **Rastinejad, F., M. J. Conboy, T. A. Rando, and H. M. Blau.** 1993. Tumor suppression by RNA from the 3′ untranslated region of α-tropomyosin. Cell **75:**1107–1117.
57. **Richler, C., H. Soreq, and J. Wahrman.** 1992. X inactivation in mammalian testis is correlated with inactive X-specific transcription. Nat. Genet. **2:**192–195.
58. **Salido, E. C., P. H. Yen, T. K. Mohandas, and L. J. Shapiro.** 1992. Expression of the X-inactivation-associated gene XIST during spermatogenesis. Nat. Genet. **2:**196–199.
59. **Schagger, H., and G. von Jagow.** 1987. Tricine-sodium dodecyl sulphate-polyacrylamide gel electrophoresis for the separation of proteins in the range from 1 to 100 kDa. Anal. Biochem. **166:**368–379.
60. **Schwartz, R. C., L. W. Stanton, S. C. Riley, K. B. Marcu, and O. N. Witte.** 1986. Synergism of v-*myc* and v-Ha-*ras* in the *in vitro* neoplastic progression of murine lymphoid cells. Mol. Cell. Biol. **6:**3221–3231.
61. **Shapiro, M. B., and P. Senapathy.** 1987. RNA splice junctions of different classes of eukaryotes: sequence statistics and functional implications in gene expression. Nucleic Acids Res. **15:**7155–7174.
62. **Shinto, Y., M. Morimoto, M. Katsumata, A. Uchida, K. Aozasa, M. Okamoto, T. Kurosawa, T. Ochi, M. I. Greene, and Y. Tsujimoto.** 1995. Moloney murine leukemia virus infection accelerates lymphomagenesis in Eμ-*bcl*-2 transgenic mice. Oncogene **11:**1729–1736.
63. **Strasser, A., A. W. Harris, M. L. Bath, and S. Cory.** 1990. Novel primitive

lymphoid tumours induced in transgenic mice by cooperation between *myc* and *bcl*-2. Nature (London) **348:**331–333.
64. **Tam, W., P. Besmer, S. H. Hughes, and W. S. Hayward.** Unpublished data.
65. **Taniguchi, T., M. J. Sullivan, O. Ogawa, and A. E. Reeve.** 1995. Epigenetic changes encompassing the *Igf2*/*H19* locus associated with relaxation of *Igf2* imprinting and silencing of *H19* in Wilms tumor. Proc. Natl. Acad. Sci. USA **92:**2159–2163.
66. **Thompson, C. B., E. H. Humphries, L. M. Carlson, C.-L. H. Chen, and P. E. Neiman.** 1987. The effect of alterations in *myc* gene expression on B cell development in the bursa of Fabricius. Cell **51:**371–381.
67. **Uberbacher, E. C., and R. J. Mural.** 1991. Locating protein-coding regions in human DNA sequences by a multiple sensor-neural network approach. Proc. Natl. Acad. Sci. USA **88:**11262–11265.
68. **van Gurp, R. J., J. W. Oosterhuis, V. Kalscheuer, E. C. Mariman, and L. H. Looijenga.** 1994. Biallelic expression of the *H19* and *Igf2* genes in human testicular germ cell tumors. J. Natl. Cancer Inst. **86:**1070–1075.
69. **van Lohuizen, M., and A. Berns.** 1990. Tumorigenesis by slow-transforming retroviruses—an update. Biochim. Biophys. Acta **1032:**213–235.
70. **van Lohuizen, M., S. Verbeek, P. Krimpenfort, J. Domen, C. Saris, T. Radaszkiewicz, and A. Berns.** 1989. Predisposition to lymphomagenesis in *pim-1* transgenic mice: cooperation with c-*myc* and N-*myc* in murine leukemia virus-induced tumors. Cell **56:**673–682.
71. **van Lohuizen, M., S. Verbeek, B. Scheijen, E. Wientjens, H. van der Gulden, and A. Berns.** 1991. Identification of cooperating oncogenes in Eμ-*myc* transgenic mice by provirus tagging. Cell **65:**737–752.
72. **Verbeek, S., M. van Lohuizen, M. van der Valk, J. Domen, G. Kraal, and A. Berns.** 1991. Mice bearing the Eμ-*myc* and Eμ-*pim-1* transgenes develop pre-B-cell leukemia prenatally. Mol. Cell. Biol. **11:**1176–1179.
73. **Wickens, M.** 1990. How the messenger got its tail: addition of poly(A) in the nucleus. Trends Biochem. Sci. **15:**277–281.
74. **Zuker, M., and P. Stiegler.** 1981. Optimal computer folding of large RNA sequences using thermodynamics and auxiliary information. Nucleic Acids Res. **9:**133–148.